

THE DEVELOPMENT OF FEM PROGRAM FOR COUPLING ANALYSIS OF THE HYPERELASTIC SOLID AND STATIC LIQUID TO SIMULATE RETINA DETACHMENT OPERATION ON AN EYEBALL

Zhi-Gang SUN* , Akitake MAKINOCHI*

* Materials Fabrication Laboratory, RIKEN
2-1, Hirosawa, Wako-shi, Saitama 351-0198 Japan
e-mail: zgsun@postman.riken.go.jp
akitake@postman.riken.go.jp

Abstract: as a fundamental study for our research, a 2D incompressible hyperelastic FEM program which employ the mixed FEM formulation is first developed and its performance is examined through several numerical experiments. Then, based on this program, a 2D coupling analysis program of the hyperelastic solid and static liquid is further developed and two numerical experiments including the trial analysis of the buckling operation on an eyeball are performed to demonstrate its effectiveness.

1.INTRODUCTION

The objective of our research is to use the FE numerical Simulation method to simulate the retina detachment operation on an eyeball, which is at present mainly based on the experiences of the surgeon in clinic. The main purpose is to predict the optimum conditions for the clinical operation. However, The eyeball is a complex three-dimensional structure consisting of both the soft solid tissues and the liquid tissues. Thus, The problem is characterized by the three-dimensional solid-liquid coupling analysis. Therefore, it is necessary to develop a numerical simulation program based on the effective finite element formulation that can reliably describe the mechanical behavior of both the solid tissues and the liquid tissues, and in particular, can succeed in performing the solid-liquid coupling analysis.

The biomechanical response of many soft tissues of the living human and animals including a few tissues of the eyeball has been investigated by the mechanical experiments [1-3]. The results showed that most of them exhibits the nonlinear-elastic mechanical behavior, such as the incompressible hyper-elasticity. On the other hand, The retina detachment operation on an eyeball is a quasi-static process in clinic, thus it is natural to idealize the liquids enclosing in an eyeball as the static liquid in FEM simulation. In this paper, corresponding to the analysis of the nonlinear elastic response of the soft tissues, a 2D incompressible hyperelastic FEM program employed the mixed FEM formulation is first developed and several numerical experiments are performed to test this program and discuss the performances of the introduced mixed element types. Then, to arrive at the main purpose of this study, a 2D solid-liquid coupling analysis program in which the liquid is treated as the static liquid is further developed based on this program. Two numerical experiments including the trial analysis of the buckling operation on an eyeball are finally presented to show its effectiveness.

This work is a fundamental study for our research.

2. THE DEVELOPMENT OF 2D INCOMPRESSIBLE HYPERELASTIC PROGRAM

In this section, corresponding to the analysis of the nonlinear elastic response of the soft tissues, a 2D incompressible hyperelastic FEM program that employ the mixed FEM formulation, in which not only the displacement but also the pressure is used as unknown variables, is first developed. Further, several numerical experiments are performed to test this program. The results used different element types are presented and compared in each case.

2.1 The mixed FEM formulation

The incompressible hyperelastic material is characterized by the stored strain energy function and incompressibility constraint condition, as expressed in the following forms respectively:

Strain energy function:

$$W = W(I_1, I_2) \quad (1)$$

Incompressibility constraint condition:

$$J = 1 \quad \text{or} \quad I_3 = 1 \quad (2)$$

where J ($J = I_3^{1/2}$) is the determinant of the jacobian matrix and I_1, I_2, I_3 are the three invariants of the right Cauchy-Green deformation tensor defined by:

$$\begin{aligned} I_1 &= 2\varepsilon_{ii} + 3 \\ I_2 &= 2\varepsilon_{ii}\varepsilon_{jj} + 4\varepsilon_{ii} - 2\varepsilon_{ij}\varepsilon_{ij} + 3 \\ I_3 &= \det(2\varepsilon_{ij} + \delta_{ij}) \end{aligned} \quad (3)$$

where ε is the Green-Lagrange strain calculated by the displacement u as follows:

$$\varepsilon_{ij} = \frac{1}{2} \left(\frac{\partial u_i}{\partial X_j} + \frac{\partial u_j}{\partial X_i} + \frac{\partial u_m}{\partial X_i} \frac{\partial u_m}{\partial X_j} \right) \quad (4)$$

However, the use of above invariants can cause the lack of the analysis accuracy. To avoid this problem, the following reduced invariants are used conventionally.

$$\bar{I}_1 = I_1 J^{-2/3} \quad \bar{I}_2 = I_2 J^{-4/3} \quad (5)$$

Thus, the strain energy function becomes:

$$W = W(\bar{I}_1, \bar{I}_2) \quad (6)$$

In our program, the Lagrange multiplier method based on the total lagrange formulation, in which the initial undeformed state is chosen as the reference configuration, is adopted. In this method, the incompressibility constraint is enforced by introducing the lagrange multiplier into the potential energy functional and Its total potential energy functional gives the following form:

$$\Phi = \int_{V_0} (W(\bar{I}_1, \bar{I}_2) + 2\lambda(J - 1)) dV - g(\mathbf{u}) \quad (7)$$

where V_0 is the volume of body in the reference configuration, λ is the Lagrange mutiplier equivalent to the hydrostatic pressure, and $g(\mathbf{u})$ is the potential energy of the external forces.

Invoking the stationarity of (7), we can obtain its variational equation:

$$\begin{aligned} \delta\Phi &= \int_{V_0} (\partial W / \partial \varepsilon_{ij} + 2\lambda(\partial J / \partial \varepsilon_{ij})) \delta \varepsilon_{ij} dV \\ &+ \int_{V_0} 2(J - 1) \delta \lambda dV - g(\delta \mathbf{u}) \\ &= 0 \end{aligned} \quad (8)$$

thus, the approximation of the analysis can be found as the stationary points.

Unlike the displacement-based finite element formulation, In mixed finite element formulation, both the displacement and the pressure are used as the unknown variables. The displacement and pressure within an element are interpolated as follows, respectively:

$$\mathbf{u}_i = \phi_N \mathbf{u}_{Ni} \quad \lambda = \varphi_R \lambda_R \quad (9)$$

where ϕ_N is the displacement interpolation function and φ_R is the pressure (Lagrange multiplier)interpolation function. While N is the number of displacement nodes and R is the number of pressure nodes within an element.

To achieve the finite element discretization, substituting (9) into (8), the following equation for one element being considered can be obtained:

$$\begin{cases} \int_{V_0} (\partial W / \partial \varepsilon_{ij} + 2\lambda(\partial J / \partial \varepsilon_{ij})) ((\partial \phi_M / \partial X_j) \mathbf{u}_{Mn} + \delta_{jn}) (\partial \phi_N / \partial X_i) dV = r_{Nn} \\ \int_{V_0} \varphi_R 2(J - 1) dV = 0 \end{cases} \quad (10)$$

where r_{Nn} is the equivalent nodal force corresponding to the $g(\mathbf{u})$ in (7).

However, equation (10) is highly nonlinear in the unknown node displacements and pressures so that it is not easy to be solved. To solve this equation we adopted the Newton-Raphson iteration scheme, which is most frequently used in nonlinear FEM analysis. The key for this iterative solution procedure is the linearization of above nonlinear equation achieved by Taylor series expansion.

Assume that in the iterative solution, the solution at the $(i - 1)$ th iteration step have been

evaluated, then a Taylor series expansion gives the incremental stiffness equation for an element at the i th iteration step in the form:

$$\begin{bmatrix} k_1^{i-1} & k_2^{i-1} \\ k_3^{i-1} & 0 \end{bmatrix} \begin{bmatrix} \Delta U^i \\ \Delta \lambda^i \end{bmatrix} = \begin{bmatrix} f u_1^{i-1} \\ f \lambda_2^{i-1} \end{bmatrix} + \begin{bmatrix} r \\ 0 \end{bmatrix} \quad (11)$$

further, by assembling the element stiffness equations, the global incremental stiffness equation can be easily obtained:

$$\begin{bmatrix} K_1^{i-1} & K_2^{i-1} \\ K_3^{i-1} & 0 \end{bmatrix} \begin{bmatrix} \Delta U^i \\ \Delta \lambda^i \end{bmatrix} = \begin{bmatrix} F U_1^{i-1} \\ F \lambda_2^{i-1} \end{bmatrix} + \begin{bmatrix} R \\ 0 \end{bmatrix} \quad (12)$$

thus, in each iteration step, the increments ΔU^i and $\Delta \lambda^i$ can be calculated in (12) and the displacements and pressures at the displacement node points and pressure node points are updated according to:

$$\begin{aligned} U^i &= U^{i-1} + \omega \Delta U^i \\ \lambda^i &= \lambda^{i-1} + \omega \Delta \lambda^i \end{aligned} \quad \omega : \text{relaxation factor.} \quad (13)$$

To achieve the correct values of U and λ , the iteration is continued until the increments become sufficiently small.

2.2 Some numerical experiments

In this program, the three types of two-dimensional mixed element are introduced i.e. the 4/1, 8/1 and 9/3 elements. Here, the 9/3 element, for example, means that the nine displacement nodes and three pressure nodes are used to interpolate the displacement and pressure within an element, respectively. On the other hand, for corresponding to the various practical analysis problems, the three types of boundary condition prescribed by the displacement, force and pressure are made applicable.

In this section, we present some simple but basic numerical examples. In the all cases, all the three types of element are used and the full Gauss numerical integration scheme is employed to evaluate the element stiffness matrix and force vector. The goals of the analyses are to examine the effectiveness of the program and to test the performances of the element types.

In Fig.1, we summarily give the models used in analyses. For the all cases, the finite element meshes for the 4/1 element is so obtained by subdividing one mesh for 8/1 or 9/1 element into four meshes, that the total displacement degrees of freedom are almost equal for the three types of element. In Fig.1, we only show the meshes for 4/1 element. Moreover, the Mooney-Rivlin material, which the stored energy function is expressed as $W = c_1(I_1 - 3) + c_2(I_2 - 3)$, with material constants: $c_1 = 1.5$, $c_2 = 0.5$ is used in each case.

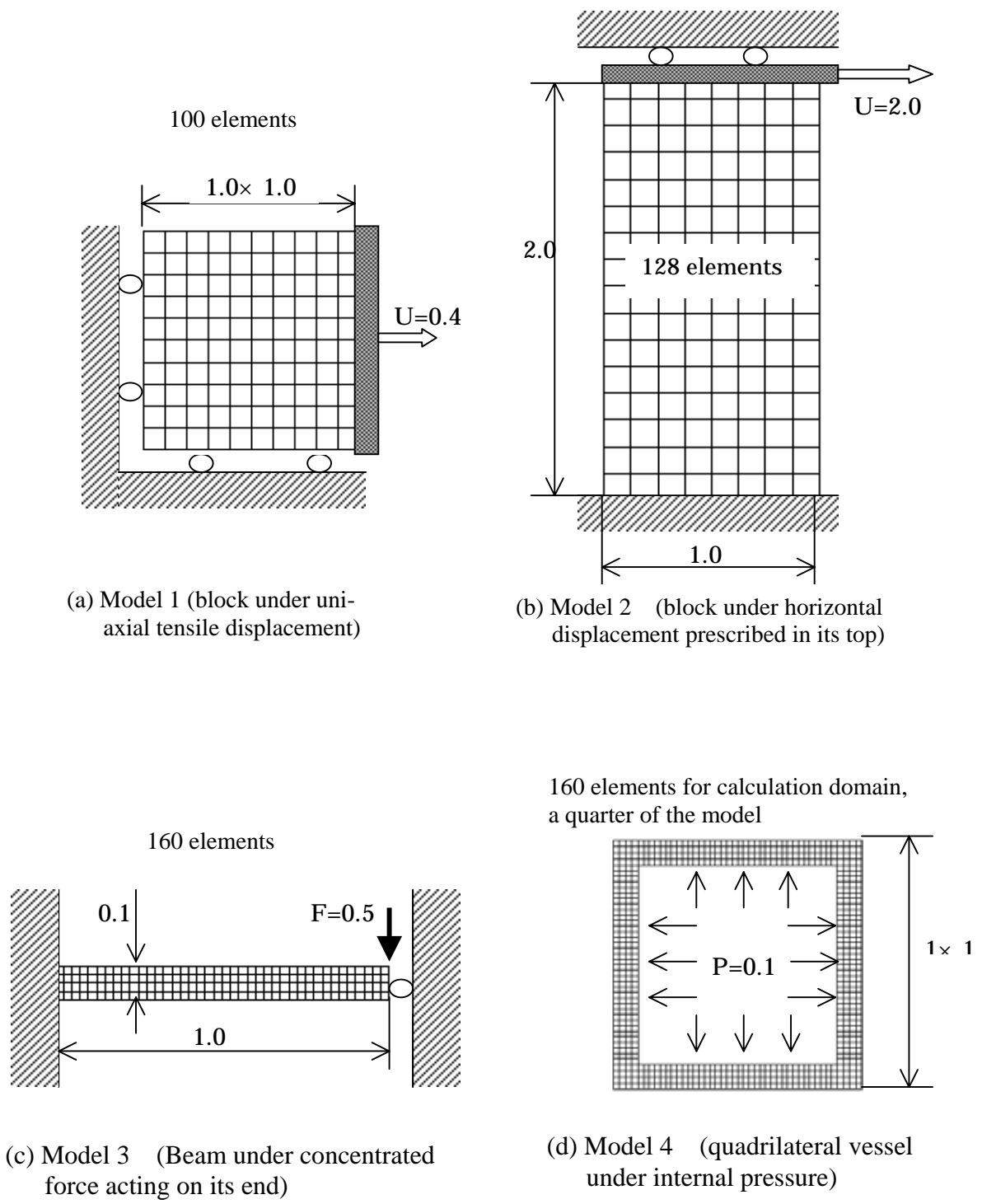


Fig. 1 Analysis models

Table 1 Calculation times and iteration solution steps

Mises

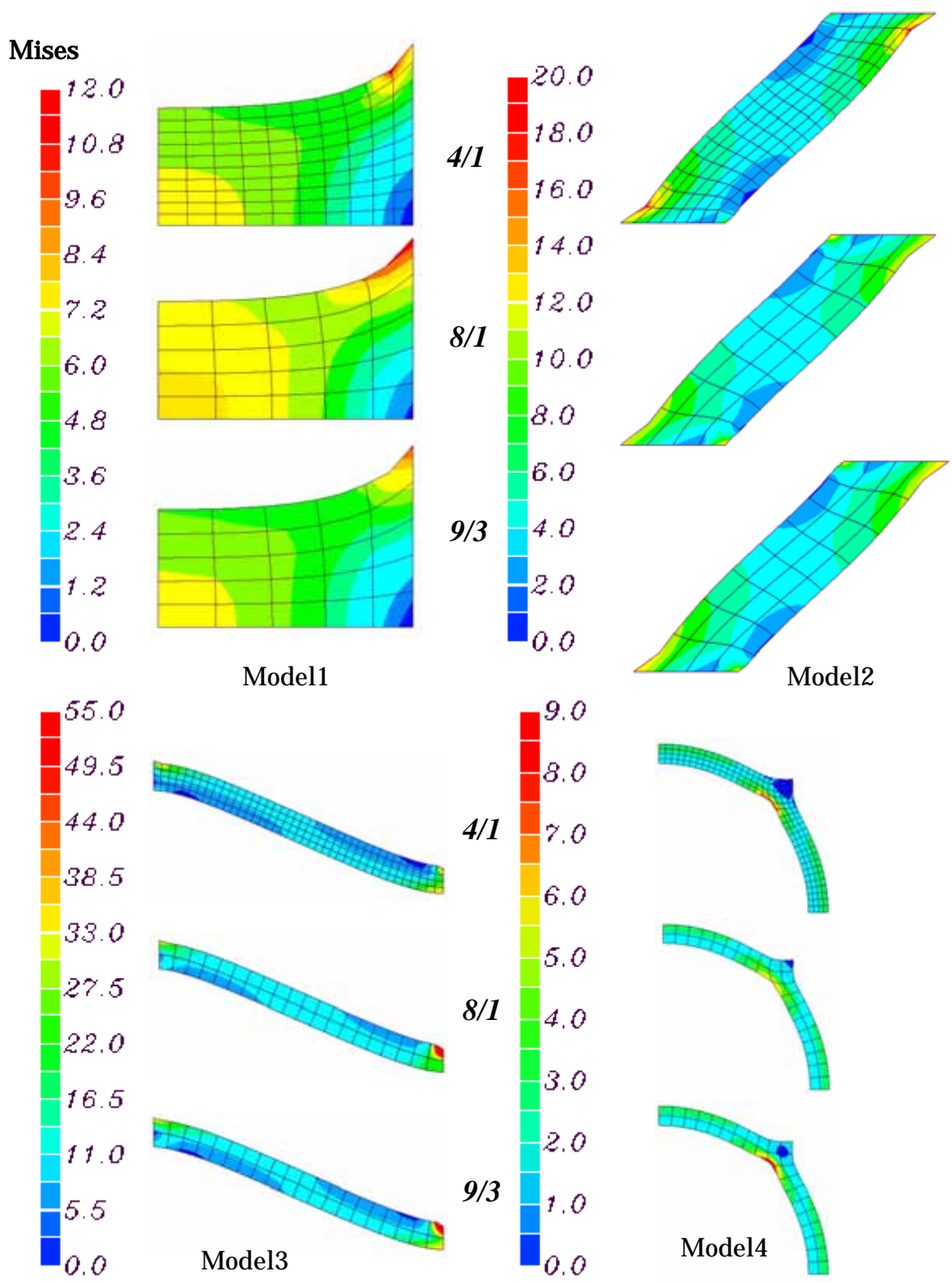


Fig. 2 Analysis results of the deformed shape and Mises stress distribution.

	Calculation times (sec.)			Iteration steps		
	4/1	8/1	9/3	4/1	8/1	9/3
Model 1	30	54	72	94	123	113
Model 2	144	246	312	319	429	371
Model 3	42	59	66	60	72	61
Model 4	144	214	246	110	121	116

The analysis results of the deformed shapes and Mises stresses are summarized in Fig. 2. We can see that in the all cases, the reasonable and satisfactory results are obtained for all the element types 4/1, 8/1 and 9/1. Further, It is observed that the results from the three element types are in good agreement in each case, except that the maximum Mises stresses are slightly different. The calculation times and iteration steps for the three element types in each case are given in Table 1. By comparing with other two element types in each case, it is obvious that either the times or the iteration steps cost for the calculations employed the 4/1 element are most small. In particular, the calculation times for the 9/1 element are over two times as much as the 4/1 element. From the above analysis results, we can conclude that the program developed here is effective and, that the 4/1 element have the best performance among the three element types, from the points of view of both the calculation efficiency and the convergence of the Newton-Raphson iteration solution.

3. THE DEVELOPMENT OF SOLID-LIQUID COUPLING ANALYSIS PROGRAM

In this section, to arrive at the main purpose in this study, a 2D solid-liquid coupling analysis program is further developed by introducing the effect of the liquid into the program developed above. Since the liquids enclosed in the eyeball can be considered as the static one for the reason mentioned in introduction, only its hydrostatic pressure caused by the volume change during deformation is taken into account in our formulation.

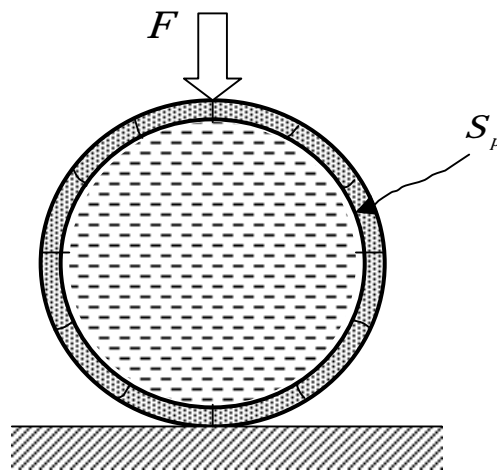


Fig. 3 Circular vessel filled with liquid under a load applied to its top

Let us consider a circular vessel filled with liquid as shown in Fig.3 which is subjected to a

force load applied to its top. It is imaginable that the pressure will occur in the liquid as the vessel is deformed by the applied load and, it will act on the inside surface of the vessel. It is assumed that the pressure is uniform through out the liquid, because it will be treated as the static liquid in our formulation. To achieve such a solid-liquid coupling analysis, thus, the problem will be how to introduce the liquid pressure into the solid part, the wall of the vessel, as the pressure boundary condition.

3.1 Finite element formulation

For convenience, here, we assume that the wall of vessel is divided into the 4/1 elements for analysis. Now, let us take out a segment of the inside surface of vessel as shown in Fig. 4, which is one edge of the any 4/1 element lay on the wall. Then, the nodal forces equivalent to the liquid pressure acting on it can be simply calculated by equally assigning the total force to each node:

$$R_1 = R_2 = \frac{1}{2} \cdot L(u_e) \cdot P(u_{s_p}) \cdot n(u_e) \quad (14)$$

where, n is the inward normal to segment, u_e denote the node displacements of the segment and u_{s_p} denote the displacements of the all nodes on the inside surface of vessel.

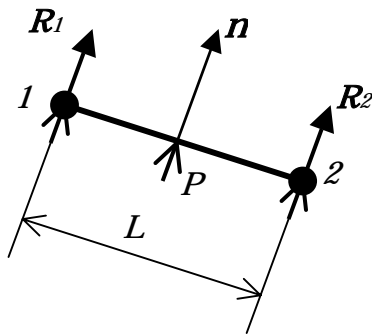


Fig. 4 A segment of the inside surface of the vessel

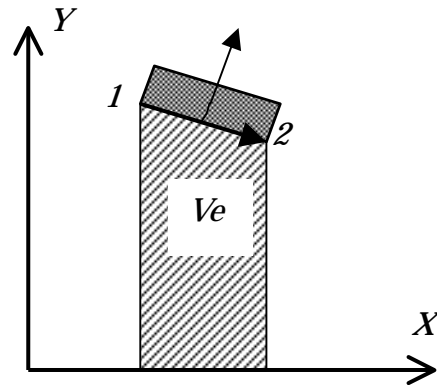


Fig. 5 Calculation of the liquid volume

Therefore, it is obvious that for calculating the equivalent forces above, it is necessary to obtain the liquid pressure. The liquid pressure can be obtained through the following procedure.

In the case of static liquid, the pressure change and the volume change always satisfies the following relation [4]:

$$\Delta P = -K \frac{\Delta V}{V_0} \quad (15)$$

where, K is the liquid buck modulus and V_0 is the liquid initial volume.

The liquid volume during deformation can be calculated by taking the summation of the volumes shown in Fig. 5 which are obtained from each segment on the inside surface:

$$V(u_{S_p}) = \Sigma V_e(u_e) \quad (16)$$

$$V_e(u_e) = \frac{1}{2}(x_2 - x_1)(y_1 + y_2) \quad (17)$$

Then, the volume change, the pressure change and the pressure can be written as follows, respectively:

$$\Delta V(u_{S_p}) = V(u_{S_p}) - V_0 \quad (18)$$

$$\Delta P(u_{S_p}) = -K \left(\frac{V(u_{S_p})}{V_0} - 1 \right) \quad (19)$$

$$P(u_{S_p}) = P_0 - K \left(\frac{V(u_{S_p})}{V_0} - 1 \right) \quad (20)$$

where, P_0 is the initial pressure of liquid.

Thus, Substituting from (20) into (14), we can obtain the equivalent forces expressed as the displacements of the all nodes on the inside surface:

$$R_1 = R_2 = R(u_{S_p}) \quad (21)$$

Further, Substituting (21) into the right-hand side of the first equation in (10), paying attention to the node correspondence, we can obtain the modified one for equation (10):

$$\left[\int_{V_0} (\partial W / \partial \varepsilon_{ij} + 2\lambda(\partial J / \partial \varepsilon_{ij})) ((\partial \phi_M / \partial X_j) \mathbf{u}_{Mn} + \delta_{jn}) (\partial \phi_N / \partial X_i) dV = \mathbf{r}_{Nn} + \mathbf{r}_{Nn}^L(u_{S_p}) \right. \\ \left. \int_{V_0} \varphi_R 2(J - 1) dV = 0 \right] \quad (22)$$

where, $\mathbf{r}_{Nn}^L(u_{S_p})$ denotes the components of R_1 or R_2 .

Using the same procedure as (12), finally, we can arrive at the global incremental stiffness equation for the solid-liquid coupling analysis:

$$\begin{bmatrix} K_1^{i-1} + K_{1L}^{i-1} & K_2^{i-1} \\ K_3^{i-1} & 0 \end{bmatrix} \begin{bmatrix} \Delta U^i \\ \Delta \lambda^i \end{bmatrix} = \begin{bmatrix} FU_1^{i-1} \\ FU_2^{i-1} \end{bmatrix} + \begin{bmatrix} R + R_L^{i-1} \\ 0 \end{bmatrix} \quad (23)$$

where, K_{1L}^{i-1} and R_L^{i-1} occurred newly in (23) comes from the liquid.

Thus, solving this equation in the same way as (12), we can obtain the solution for the coupling analysis problem that we expected.

3.2 Some numerical experiments

To examine the effectiveness of the formulation for solid-liquid coupling analysis presented above, two numerical experiments are carried out. For these analyses, the 4/1 element is employed because it has been demonstrated in preceding section that this element type is best one among the three element types introduced into our program.

3.2.1 analysis of the quadrilateral vessel filled with liquid under the pressures applied to both its top and its bottom

A quadrilateral vessel filled with liquid is subjected to the uniform pressures applied to both its top and its bottom. In order to examine easily the reasonableness of the analysis result, the analysis of a hollow quadrilateral vessel subjected to the same pressures is performed simultaneously. The analysis models are shown in Fig. 6. Here, from the geometrical symmetry, only a quarters of the models with 160 elements are used for analyses. Moreover, the Mooney-Rivlin material descriptions are used to model the walls of vessels, with material constants $C_1 = 1.5$, $C_2 = 0.5$ and, the bulk modulus of the liquid is assumed to be 2083.3MPa , which is equal to the water.

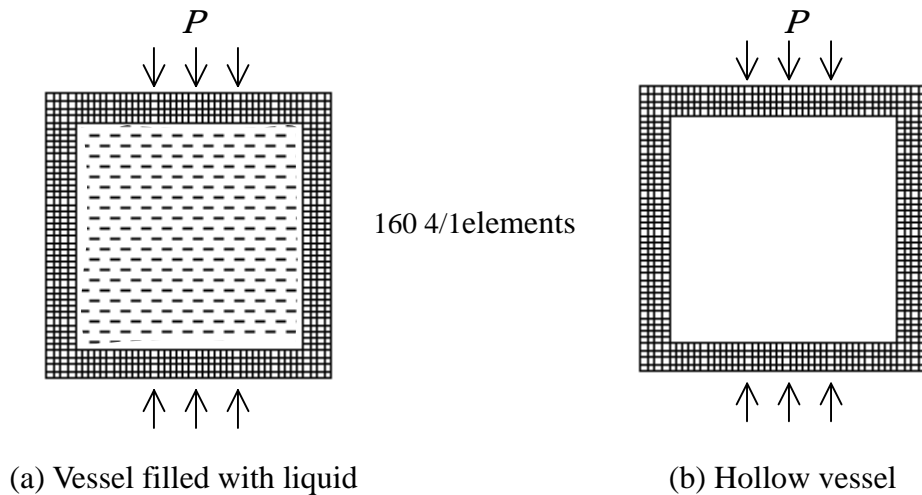


Fig. 6 Analysis models for quadrilateral vessel subjected to pressures applied to both its top and bottom.

The analysis results of the deformed shapes and Mises stresses obtained in the two cases are given in Fig.7. It is seen that the results are remarkably different. In the case (a), the vessel underwent much larger deformation, stress and decrease in the thickness of the wall, comparing with case (b), because the volume of the liquid enclosed in vessel was almost unchanged. While the pressure needed to achieve such a deformation for the case (b) are 20 times as smaller as for the case (a). Obviously, the results obtained in the analysis of case (a) are desirable and satisfactory. Hence it can be concluded that the formulation for solid-liquid coupling analysis presented above is effective.

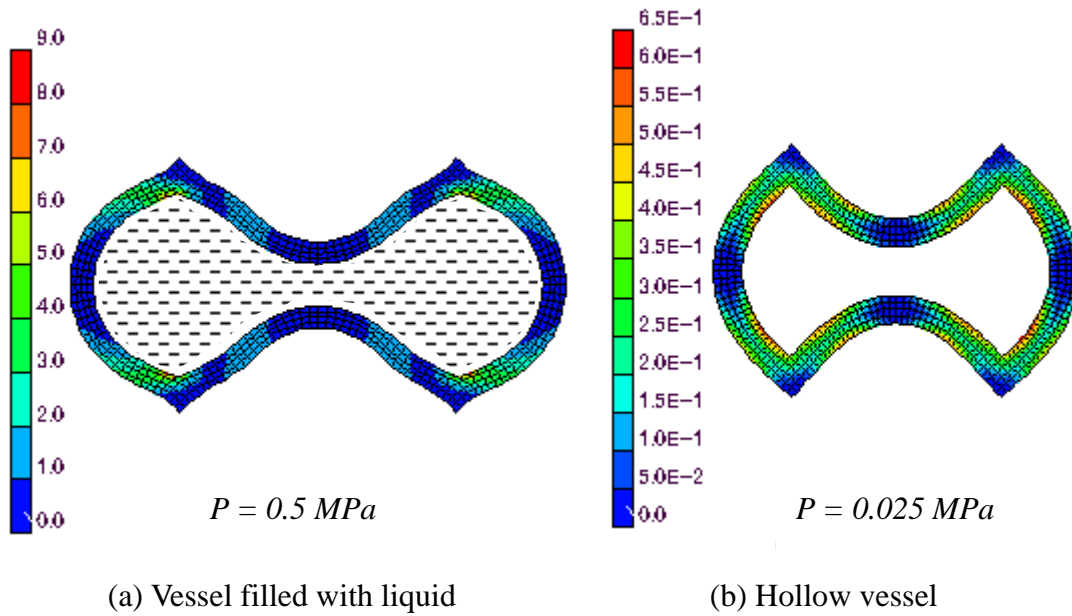


Fig. 7 Analysis results of the deformation shapes and Mises stresses using the models shown in Fig. 6.

3.3.2 Analysis of the buckling operation on an eyeball

As have been mentioned in introduction, the purpose of our research is to simulate the retina detachment operation on an eyeball in order to predict the optimum conditions for clinical operation. Here, the analysis of the buckling operation on an eyeball is tried, since it is most frequently performed in clinical treatment for eyeball retina detachment. Although actually the eyeball have the complex 3D structure so that the 3D analysis is needed, it is expected that qualitative somewhat useful for the operation will be given by the 2D analysis. In this analysis, we only tried to qualitatively investigate the influence of the initial inner pressure on the shape of the eyeball buckled up, because the effect of the inner pressure on such operation have been recognized from the clinical operation.

The finite element division and tissue division used for analysis are given in Fig. 8. From the geometric symmetry, only a quarter of the model with 115 elements are used for analysis. The Neo-Hooke material model, which the stored energy function is expressed as $W = c_1(I_1 - 3)$, is used for the all soft tissues, and the material constants are given in Table 1, which are obtained by transforming the Young's moduli used in the reference [5]. The buck modulus: $2083.3MPa$ is used for the liquids enclosed in two closed domains inside the eyeball. Further, the prescribed displacement is applied to the eyeball to simulate the buckling process as shown in Fig. 8.

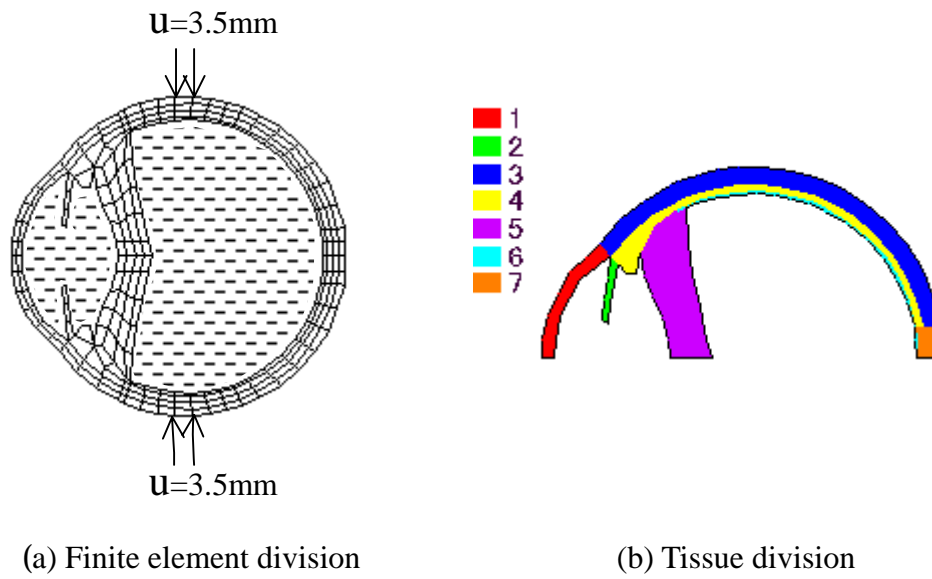


Fig. 8 Analysis model for buckling operation on an eyeball

Table 1 Material constants of tissues

	1- cornea	2-iris	3-sclera	4-choroid	5-vitreous	6-retina	7-optic nerve
C_I	0.033	0.0083	0.083	0.0083	0.00002	0.0083	0.0083

The two analyses for which the different initial inner pressures are used are carried out. In the case1, the zero inner pressure is assumed although in fact such a state does not exist. The analysis result is shown in Fig. 9. It can be seen that this analysis resulted in a deformed shape with the shrunk rear and it is different from the actual shape of eyeball buckled up, which have been known from the clinic observation. On the other hand, in the case 2, the analysis is performed in two steps, i.e. in the first step, a 6.0mmHg(0.0008MPa) pressure are applied to the surfaces of the two closed domains inside eyeball as the pressure boundary condition to make the inner pressure. Then, in the second step, it is turned to the solid-liquid coupling analysis with this pressure as initial inner pressure by imposing the prescribed displacement. The result is shown in Fig. 10. Obviously the deformed shape of eyeball is different from that obtained in case1, but it approximately agree with the actual one. Thus, through these analyses, it is qualitatively confirmed that the initial inner pressure is one factor to influence the result of the buckling operation on the eyeball.

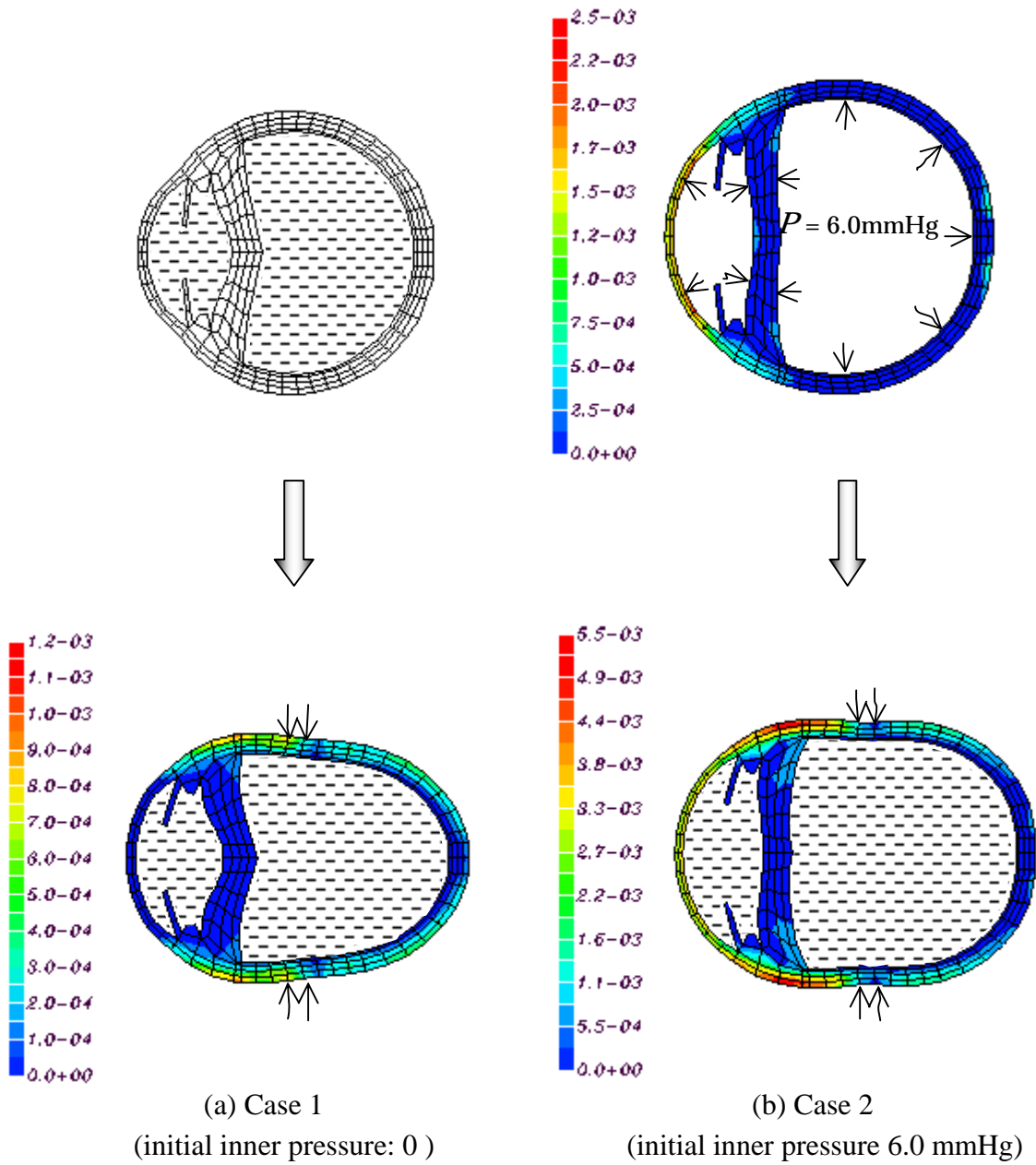


Fig. 9 Analysis results of the deformed shapes and Mises stresses for the buckling operation on an eyeball

4. CONCLUSIONS

In this paper, Corresponding to the soft tissues of the eyeball, a two-dimensional incompressible hyperelastic FEM program was first developed. The Lagrange multiplier method, which is one of the mixed FEM, was employed in this program to impose the incompressible constraint. The three types of mixed element i.e. the 4/1, 8/1 and 9/3 elements, were introduced into this program in order to discuss the influence of element types on the accuracy and efficiency of the analysis and to give the best choice of element for analysis. For corresponding to the various practical analysis problems, the boundary conditions prescribed by the displacement, force and pressure were made applicable. Using this program, several numerical experiments were performed. The results showed that this program is effective, and that the 4/1 element can give the best performance among the three element types from the points of view of both the accuracy and the efficiency of the analysis. Finally, to arrive at the main purpose in this study, A solid-liquid coupling analysis program was further developed based on the above program. Since the retina detachment operation on an eyeball is a quasi-static process, the liquid was treated as the static one in this program. Two numerical tests including the analysis of the buckling operation on an eyeball, which is most frequently performed in clinic to treat the retina detachment, was carried out. From the tests, it was shown that the results are satisfactory and, it was qualitatively demonstrated that the initial inner pressure of the eyeball is one factor to influence the effect of the operation.

As have been mentioned, this work is a fundamental study for our research. It would be continued to develop the three-dimensional coupling analysis program by expanding the two-dimensional program developed here in the future.

REFERENCE

1. B. Jue and D.M.Maurice, The mechanical properties of the rabbit and human cornea. *Journal of Biomechanics*, **19**, 847-853(1986).
2. D.A.Hoeltzel, P.Altman, K.Buzard, K.I. Choe, Strip extensometry for comparison of the mechanical response of bovine, rabbit, and human corneas, *ASME Journal of biomechanical engineering*, **114**, 202-215(1992).
3. Y.C.Fung, *Biomechanics: Mechanical properties of living tissues*. Springer-Verlag(1981).
4. 富田 幸雄, *流体力学序説*, 養賢堂 .
5. 矢部比呂夫、川口龍平, *眼球の外力による損傷過程のシミュレーション*, 計算生体力学研究計画化調査報告書(理研), 1998, 103 .